ECJSE

Research Paper

Investigation of the Impact of Airfoil Geometry Alteration on Horizontal Axis Wind Turbine Performance by CFD Method

Hakan İNAN[1a], Mahmut KAPLAN[2b]

[1]Department of Mechanical Engineering, Institute of Science, Amasya University, Amasya/Türkiye
[2]Department of Machine and Metal Technology, Naci Topcuoglu Vocational High School, Gaziantep University, Gaziantep/Türkiye
mahmutkaplan@gantep.edu.tr

Abstract: As a promising source for sustainable energy, a wind turbine transforms the wind kinetic energy into electrical energy. In wind turbines, the geometry of the airfoil affects the magnitude of the aerodynamic forces on the blade surfaces. In the present work, the influence of the geometrical shape of the standard NACA 63-415 airfoil on the blade performance was investigated with the SST k-ω turbulence model using ANSYS Fluent at different wind speeds (4-16 m/s). The CFD results of the standard airfoil were verified by experimental work. In the first step, NCLS30 and NCLSUS 30 airfoils were generated by modifying the surface shape of the standard airfoil. In the second step, the solid blade models were created by calculating the optimum chords and twist angles for a design attack angle of 7°, design tip speed ratio of 7 and blade length of 20 m at 1 m intervals along the blade using SOLIDWORKS program. The highest power coefficient (C_P) value of 0.511 was achieved with the NCLSUS 30 blade at 16 m/s wind speed of and the C_P of the blade model increased by 10.62% in comparison to the standard NACA 63-415 blade. The peak blade velocity for the NCLSUS 30 blade was 7.2% higher than that with the standard blade model. The new blade models introduced in this study is thought to help future research related to the wind turbine blade design.

Keywords: Wind turbine, CFD method, airfoil surface geometry, blade model, aerodynamic performance

1. Introduction

Renewables are more important today than even before owing to depleting fossil fuel reserves, high fossil fuel prices, energy security concerns and climate change in the world. Turkey has promising wind energy potential [1]. Since the wind is an abundant, freely available and clean energy source, there is an increasing trend towards development of wind turbine technology. Wind turbines are devices that produce clean electricity from the wind's kinetic energy. The collision of the air flow with the turbine blades induces rotational motion, which subsequently leads to the conversion of the kinetic energy of the air into mechanical energy. To improve the maximum turbine efficiency, it is necessary to develop new blade design approaches and lighter materials [2]. On the other hand, turbine blades made from complex composite materials represent a specific challenge due to the requirement of specific processes for recycling [2]. Turbine blades are vulnerable to failure related to harsh environment, constantly varying loads by wind, extreme temperature, erosion and corrosion [3]. Therefore, the selection of blade material is very important in designing the wind turbine blades. Since blade geometry has an effect on the load that applied to the blade, geometric design also appears to be an important factor towards eliminating mentioned challenges. Modern wind turbines are grouped according to the rotation orientation of turbine blades in two types: horizontal-axis wind turbines (HAWT) and vertical-axis wind turbines (VAWT) [4]. The geometry and dimensions of the blades affect the performance of the HAWT blades [5]. The cross section of the blade is called an airfoil whose shape is curved. The pressure difference between the two airfoil parts generates lifting

force causing blades rotation. The lift force (F_L) is perpendicular to the flow direction from the airfoil lower surface to the upper surface, whereas a drag force (F_D) occurs parallel to the flow direction [6]. The main aim of the curved upper and lower surfaces is to minimize drag forces induced by the air friction with the surface of the blade. The lift and drag coefficients C_D and C_L (non-dimensional drag and lift) are equal to the drag and lift force divided by the product of free stream velocity and area, respectively. The aerodynamic efficiency of the standard airfoil can be improved by changing its geometry.

Recently, different studies have been performed on modelling of wind turbine blades and improving the performance characteristics of the blades using CFD method [7-20]. These works can be divided into two groups. In the first group, blades are constructed employing a single airfoil with a constant chord. In the second group, blades are generated employing different airfoils from the root to the tip. The tangential speed of the blade reaches its maximum in the blade tip then diminishes by moving to the root. The tip speed ratio (λ) calculated the ratio between the tip speed of the blade and the wind speed is very important parameter for the blade design. Some researchers observed performance of a three-dimensional blade geometry which is divided into sections [9, 10, 13]. In this method, the optimum twist angles and chord lengths in all blade sections are calculated using the blade number, rotor radius and attack angle for a fixed λ [10].

Krogstad and Lund [7] carried out combined experimental and computational investigation to examine the aerodynamic features of a small scale turbine model with 0.9 m diameter generated using NREL (the National Renewable Energy Laboratory) S826 airfoil at λ=0-12. Turbine performance was simulated employing CFD method with ANSYS Fluent. The results based on high-resolution CFD simulation demonstrated that the computed thrust coefficient (C_T) values in good agreement with experimental C_T values for λ<9 whereas the estimated power coefficients (C_P) values had good consistency with the experimental C_P values for λ<6. It was found that the observed over prediction for higher λ was owing to rotational lift enhancement and partly by three-dimensional impacts induced by transition. The results at the model scale assured that accurate estimations of turbine performance at full-scale conditions were also possible by means of CFD calculations.

Eltayesh et al. [16] conducted an experimental and numerical study of the influence of various blade numbers (2-6) on the aerodynamic efficiency of a small scale HAWT for λ=0-14 and 6-8 m/s wind speed. The computational domain of the blades was produced by ANSYS ICEM CFD software. The calculation results performed employing SST k-ω turbulence model illustrated that the model correctly predicted the C_P values obtained from the experiment for different λ and wind speeds. They found that the C_P reduced with an increase in the number of blade resulted in increasing torque and friction losses. Therefore the highest C_P was achieved with 3 blade turbine despite the fact that vortices and flow separation are stronger for the 3 blades. They also reported that the variation of λ was less sensitive and C_P-λ curve got wider with 3 blade configuration.

Gorgulu et al. [18] analysed the aerodynamic characteristics of 3D NACA 0009 airfoil model with 111 mm chord and span lengths at angle of attack (α) of 0°-15° using ANSYS Fluent software. Simulation results gained employing the k-ω turbulence model showed that C_L increased upto α=10° and then it had a decreasing trend because of reducing pressure difference between the lower and upper parts, whereas C_D increased continuously by increasing α thanks to increasing the flow separation. The best performance was achieved at α=5° and the highest L/D ratio was obtained at this angle of attack. Yossri et al. [19] observed the impact various airfoils (NACA 4415, NACA 4412, NACA 0015, NACA 0012) and three-bladed turbine models constructed using these airfoils with a rotor diameter between 50-100 cm on the power output of a small scale HAWT at 4 m/s wind speed and α=0°- 8°. 2D and 3D CFD simulations were conducted using Comsol Multiphysics software. The result of the two-dimensional analysis showed that the maximum C_L/C_D ratio was obtained with the NACA 4412 airfoil and this airfoil improved the turbine aerodynamic performance. Then they created

solid blade using the airfoils. The CFD result of 3D blade model generated using the SOLIDWORKS software demonstrated that the turbine torque and power increased with an increase in the rotor diameter for all examined blade models and the highest torque and power was obtained with the NACA 4412 blade.

Ji et al. [20] reported the influence of different wind speeds (7, 10 and 20 m/s) on the aerodynamic features of HAWT using the wind turbine blade model formed by the NREL S809 airfoil. Performance analysis of 3D blade model was done employing ANSYS Fluent solver with the transition SST and SST k-ω turbulence models. They examined that the computed pressure coefficient values gave good agreement with measurements for 7 and 10 m/s at the blade root, middle and tip sections. It was found that the capability of the transition SST and SST k-ω turbulence model to estimate the measured data decreased with a further increase in wind speed because larger flow separation occurred near the blade root with a higher speed (20 m/s).

From review of the available literature related to the blade design for performance enhancement of HAWT, it is apparent that there are many parameters such as the blade cross-sectional shape, number of blade, blade diameter, λ, α and wind speed affect the efficiency and power of HAWT. Most of computational studies were conducted for analysis of a blade model developed using standard airfoil but a few investigations included new airfoil blade models. The objective of the current study is to assess the impact of the new airfoils created by modifying the shape of the standard NACA 63-415 airfoil on the performance of HAWT blade.

2. Material and Method

To evaluate the model accuracy, the C_L curve as a function of the attack angle (0˚-20˚) for the standard NACA 63-415 airfoil is generated using ANSYS Fluent software with the SST k-ω turbulence model for a Reynolds number 1.6×10^6 [22]. Figure 1 illustrates that the numerical C_L values gained with numerous calculations give good agreement with the measured data of Bertagnolio et al. [23].
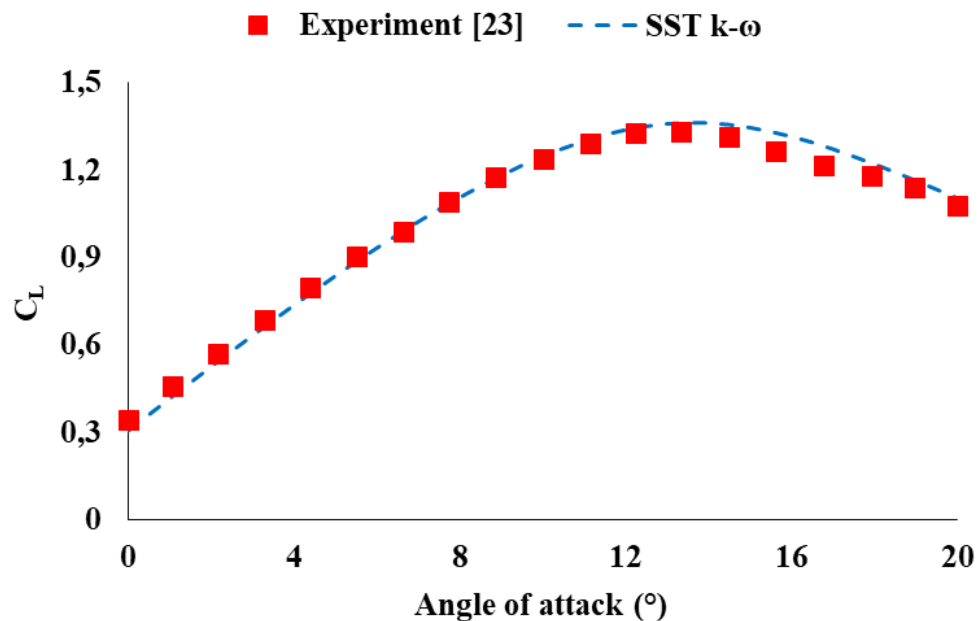
Figure 1. Comparison of calculated and experimental C_L values

Two basic steps are used to develop the wind turbine blade model. In the first step, NCLS 30 and NCLSUS 30 airfoils are created by altering surfaces of the standard NACA 63-415 airfoil, as

illustrated in Figure 2. NCLS 30 is produced by reducing y coordinate of the lower surface of the standard airfoil by 30%. NCLSUS 30 is generated by reducing y coordinate of lower and upper surfaces of the standard airfoil by 30%.
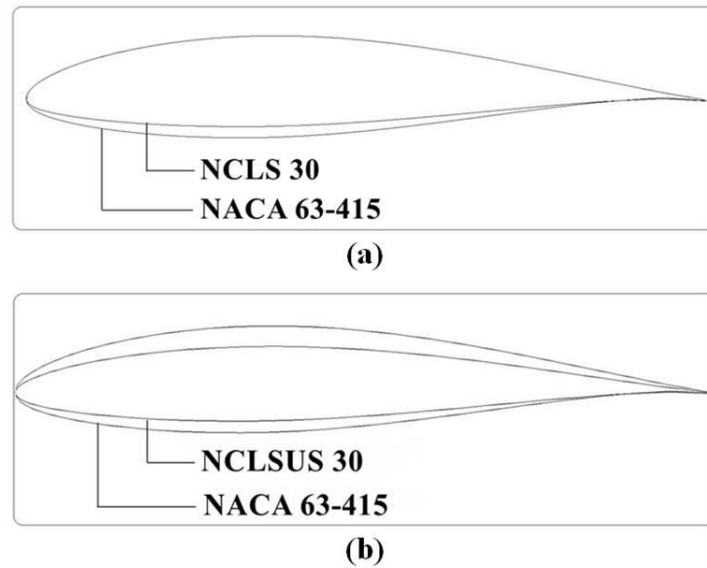
Figure 2. Airfoils produced by changing the surface geometry of the standard NACA 63-415 airfoil: (a) NCLS30, (b) NCLSUS 30

In the second step, new blades are to be designed using standard NACA 63-415 and new aerofoils (NCLS30 and NCLSUS30). For each airfoil section located along the blade length, the optimum chord length and twist angle were calculated as [10]:

$$c = \frac{1}{z} \cdot \frac{16\pi}{C_L} \cdot r \cdot \sin^2 \left[\frac{1}{3} \cdot arctan \left(\frac{R}{\lambda_{design} \cdot r} \right) \right] \tag{1}$$

$$\theta = \frac{2}{3} arctan \left(\frac{R}{\lambda_{design} \cdot r} \right) - \alpha_{design} \tag{2}$$

Here c is the chord length, z is number of blade, R is the rotor radius, r is a distance from the hub, and θ is twist angle. α_{design} and λ_{design} are the design attack angle and tip speed ratio. In the calculations, $z=3$ and $R=20$ m. In a previous study [22], it was seen that the highest C_L/C_D was obtained with NCLS 30 airfoil at α approximately equal to 7°. Therefore, $\alpha_{design} = 7°$ is chosen. In the literature [7, 10, 24], it was determined that the optimum λ value for a three bladed turbine is in the range of 6-8. Thus, $\lambda_{design}=7$ is selected in the present work. Computed c and θ values for Standard NACA 63-415, NCLS 30 and NCLSUS 30 blades are given in Table 1.

In order to generate curved blade geometry in SOLIDWORKS, the blade is divided into sections and the airfoil at each section located at 1 m intervals along the blade length. Then, each airfoil with an optimum chord length is rotated around the specified point using an optimum twist angle in Table 1.

Table 1. Optimum c and θ values for standard NACA 63-415, NCLS 30 and NCLSUS 30 blades

Sections	r (m)	θ (°)	c (m)		
			NACA 63-415	NCLS 30	NCLSUS 30
Hub	0	0	1	1	1
Section 1	1	40.13997	2.61299	2.58685	2.83794
Section 2	2	29.67199	3.23458	3.20223	3.51305
Section 3	3	22.06855	3.08766	3.05677	3.35347
Section 4	4	16.69179	2.75458	2.72702	2.99172
Section 5	5	12.82992	2.42253	2.398296	2.63108
Section 6	6	9.97556	2.13608	2.11471	2.31997
Section 7	7	7.80233	1.89818	1.87919	2.06159
Section 8	8	6.10255	1.70179	1.68476	1.84829
Section 9	9	4.74172	1.53880	1.52341	1.67127
Section 10	10	3.63026	1.40229	1.38826	1.52301
Section 11	11	2.70685	1.28679	1.27392	1.39757
Section 12	12	1.92833	1.18806	1.17618	1.29034
Section 13	13	1.26360	1.10287	1.09184	1.197820
Section 14	14	0.68975	1.02872	1.01842	1.11728
Section 15	15	0.18953	0.96365	0.95401	1.04661
Section 16	16	-0.25022	0.90614	0.89707	0.98415
Section 17	17	-0.63975	0.85497	0.84641	0.92857
Section 18	18	-0.98712	0.80916	0.80107	0.87882
Section 19	19	-1.29878	0.76794	0.76026	0.83405
Section 20	20	-1.57993	0.73065	0.72334	0.79356

The axis formed by connecting these points on the sections is called the bending axis. In this study, the bending axis point was determined as 25% of the chord length in all turbine blade models. After that, the blade models were created using the SOLIDWORKS loft command with guide curves.

Figure 3 shows the rotation of standard NACA 63-415 airfoils with the calculated optimum chord lengths and the loft guide curves of the blade.

The blade model drawn in the SOLIDWORKS program was imported into ANSYS DesignModeler of the Fluid Flow Analysis System in the ANSYS Workbench platform using a parasolid file. Only 120° of the computational fluid domain including one blade is simulated owing to the rotational symmetry as seen in Figure 5a. In ANSYS Meshing, an unstructured tetrahedral mesh was applied for a single blade and the periodic boundary conditions imposed to account for the other two blades in Figure 5 (a). In order to achieve a finer boundary layer analysis near the blade surface, the local inflation was applied as shown in Figure 5 (b). The smooth transition is specified to adjust inflation option In ANSYS Meshing. The number of inflation layers is 5 and the value of the growth rate is 1.2. In all calculations, the Pressure-Based Solver type was chosen as the solver type because the Mach number was below 0.3 in the examined velocity range. The finite volume method is employed to discretize conservation equations in the ANSYS Fluent CFD software. The discretized equations are solved using the coupled algorithm. Least Square Cell-Based method was used to calculate the gradients. In the calculations, the convergence criterion was taken as 10^{-5} for the residuals.
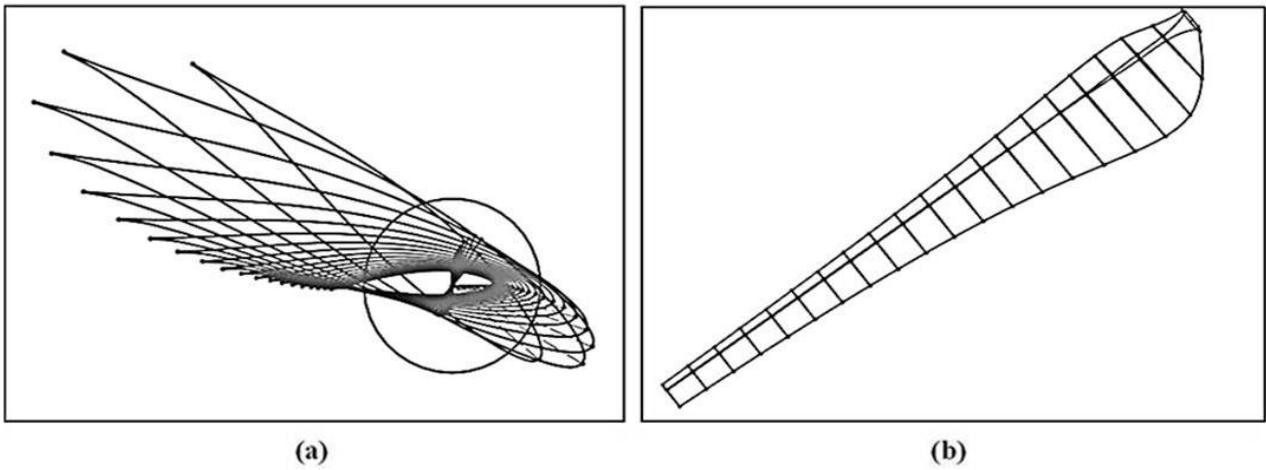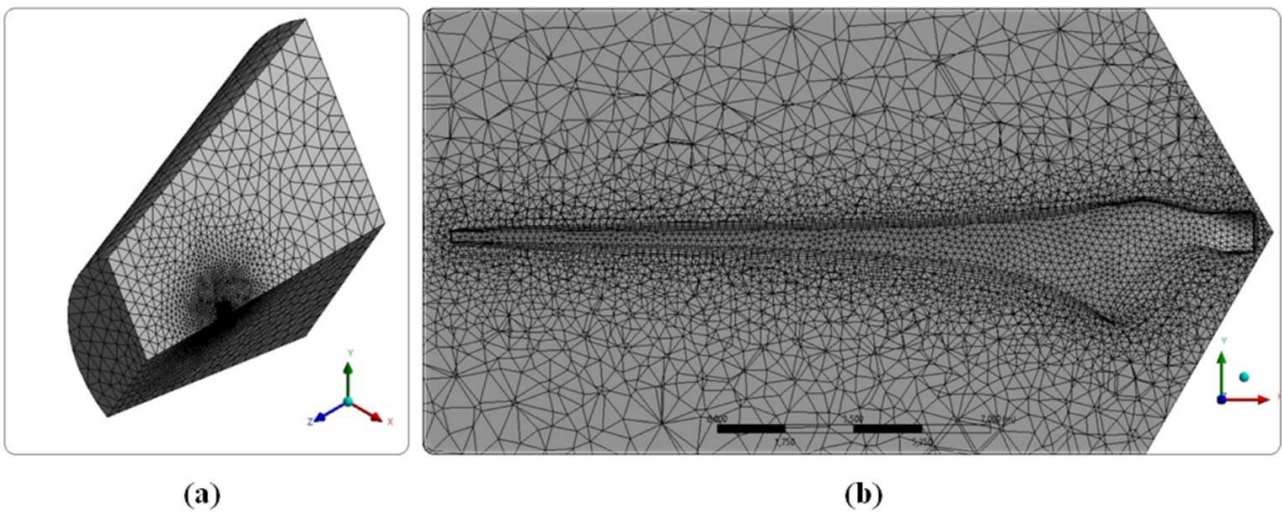
Figure 3. Producing the standard NACA 63-415 blades: a) rotation of the airfoils b) the blade guide curves

Figure 4 shows the NCLS 30 and NCLSUS 30 blades produced with the same method.
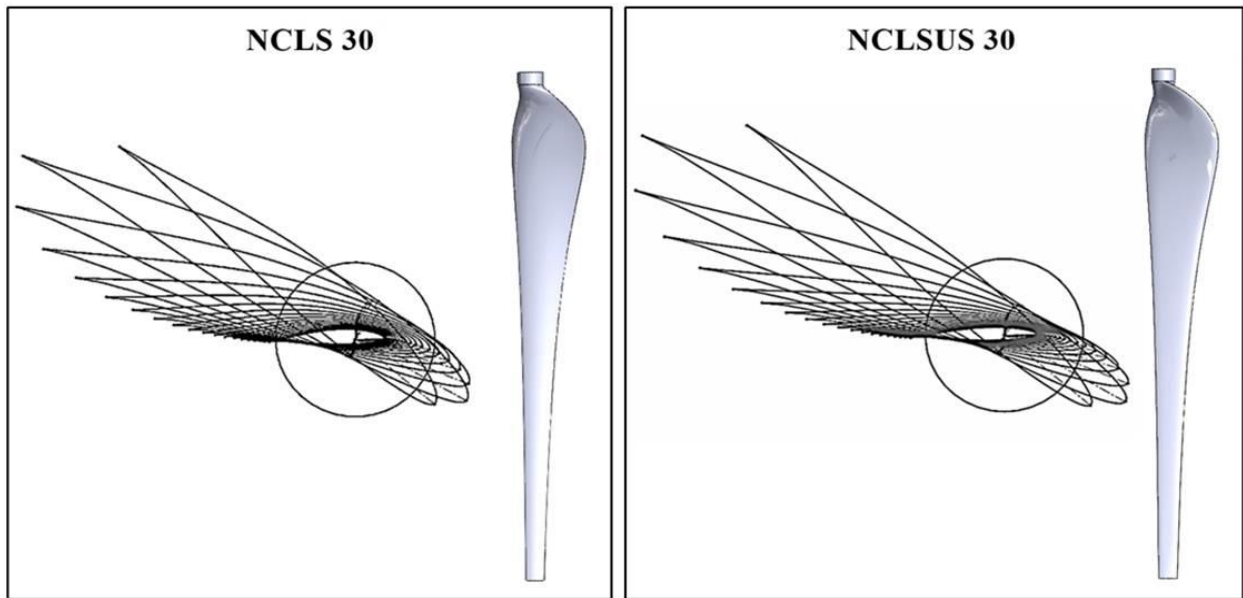
Figure 4. NCLS 30 and NCLSUS 30 blades

Figure 5. a) Unstructured grid for the flow domain b) the inflation around the blade surface

2.1 Turbulence Model

Shear-Stress Transport (SST) k-ω turbulence model was employed for computational analysis of the flow around the blade because a previous 2D study [22] showed that the SST k-ω turbulence model had better accuracy than the Spalart-Allmaras turbulence model. The SST k-ω model has two equations including turbulence kinetic energy (k) and specific dissipation rate (ω). It is formed by blending of k-ε and k-ω turbulence models [25].

This model behaves like k-ε and k-ω turbulence models in the free-flow and near-wall viscous regions, respectively. This model gives better results for separated flows, free shear flows and complicated adverse pressure gradient flows comparing to other Reynold Averaging Navier Stokes (RANS) models with turbulent viscosity approximation. The k and ω transport equations are given in Equations 3 and 4, respectively.

$$\frac{\partial}{\partial_t}(\rho k) + \frac{\partial_k}{\partial_{x_i}}(\rho k u_i) = \frac{\partial}{\partial_{x_j}}\left(\Gamma_k \frac{\partial_k}{\partial_{x_j}}\right) + G_k - Y_k + S_k \tag{3}$$

$$\frac{\partial}{\partial_t}(\rho \omega) + \frac{\partial_k}{\partial_{x_i}}(\rho \omega u_i) = \frac{\partial}{\partial_{x_j}}\left(\Gamma_\omega \frac{\partial_\omega}{\partial_{x_j}}\right) + G_\omega - Y_\omega + D_\omega + S_\omega \tag{4}$$

Here Γ_k and Γ_ω, are the effective diffusivity for k and ω, respectively. G_k is the formation of k because of the mean velocity gradient and G_ω is the formation of ω, respectively. Y_k and Y_ω represent the turbulence dissipation of k and ω, respectively. D_ω denotes the cross-diffusion term. S_k and S_ω indicate user-defined source terms. [26].

2.2 Boundary Conditions

Boundary conditions of the computational domain are shown in Figure 6. The air passing through the blade is supposed to be continuous, turbulent and incompressible.
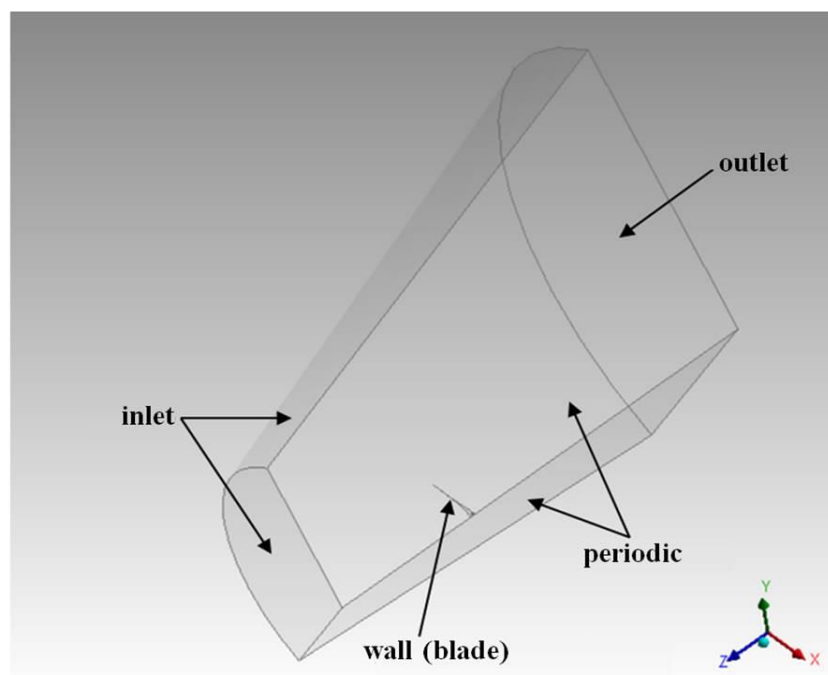
Figure 6. Boundary conditions

The velocity inlet boundary condition is employed at the flow inlet. In this study, the air inlet velocity is in the range of 4-16 m/s. The pressure boundary condition is set at the outlet. The air pressure is atmospheric. Turbulent viscosity ratio of 10 and turbulence intensity of 5 are chosen for the inlet and outlet. The flow is supposed to be cyclically periodic to reduce the grid number elements and computation time. So, periodic boundary conditions are used to two surfaces having a periodically repeating nature as shown in Figure 6. The wall boundary condition is specified to the surfaces of the blade. No slip wall condition was applied for the blade walls which are considered as smooth in all the calculations.

3. Results and Discussion

3.1 Influence of the modification of the aerofoil geometry on the blade performance

In this section, performance of new turbine blades was examined by varying wind speeds (4-16 m/s). In the wind turbine, the maximum available power is gained at specific wind speed when all wind power flowing into the turbine blades is extracted. In practice wind turbine cannot reach this power. Therefore, a power coefficient (C_P) which equals the ratio between the actual power gained by the wind turbine and the maximum available power is defined to measure how efficiently extracting wind energy.

$$C_P = P/(0{,}5\rho\pi R^2 V^3) \tag{5}$$

$$P = T\omega \tag{6}$$

where P is power produced power by the wind turbine. T and ω represent the torque and rotational speed. Figures 7 and 8 show the torque and power values calculated by CFD analysis of the standard NACA 63-415 NCLS 30 and NCLSUS 30 blades at the wind speed of 4 -16 m/s. Torque and power increased with an increase in the wind speed for all blades as seen in Figures 7 and 8.
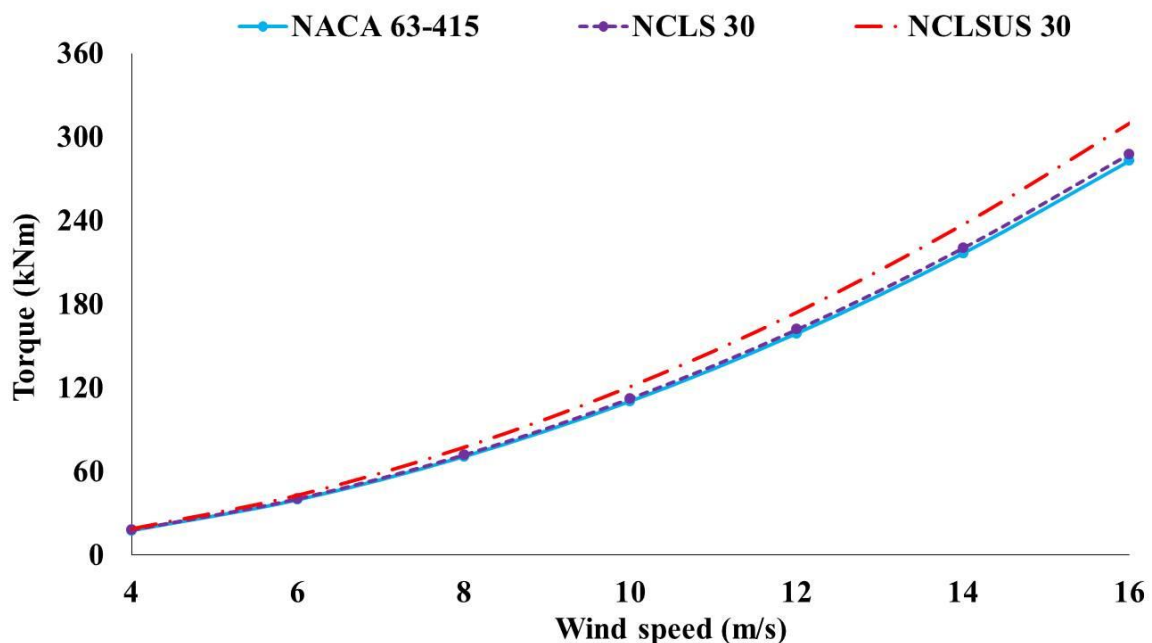
**Figure 7.** Comparison of torque-wind speed curves of NACA 63-415, NCLS 30 and NCLSUS 30 blades

The maximum torque and power were obtained at 16 m/s wind speed. Compared to other blades,

torque and power increased significantly after 10 m/s wind speed with the NCLSUS 30 blade. It was observed that the maximum torque and turbine power were obtained at 16 m/s with the NCLSUS 30 blade. As seen in Figure 8, 1545 kW turbine power was obtained with the standard NACA 63-415 blade at this speed, while 1693 kW turbine power was obtained with the NCLSUS 30 blade.
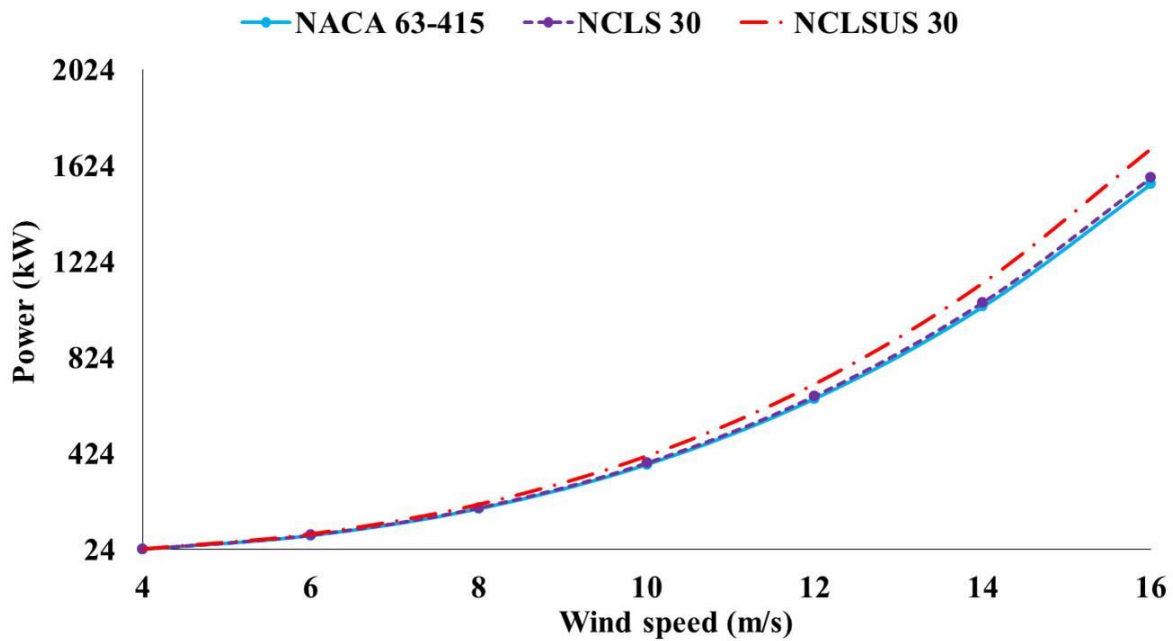
Figure 8. Comparison of power-wind speed curves of NACA 63-415, NCLS 30 and NCLSUS 30 blades

Since the maximum power was obtained at 16 m/s wind speed in all blades, the impact of new turbine blades on the C_P value was examined at this speed. Figure 9 shows the comparison of the C_P values calculated at 16 m/s wind speed of the standard NACA 63-415, NCLS 30 and NCLSUS 30 blades. In Figure 9, it is illustrated that the new blades enhance the power ratio compared to the standard NACA-63-415 blade and the peak C_P as 0.51 was obtained in the NCLSUS 30 blade. The C_P value of the NCLSUS 30 blade has increased by 10.62% compared to the standard NACA 63-415 blade.
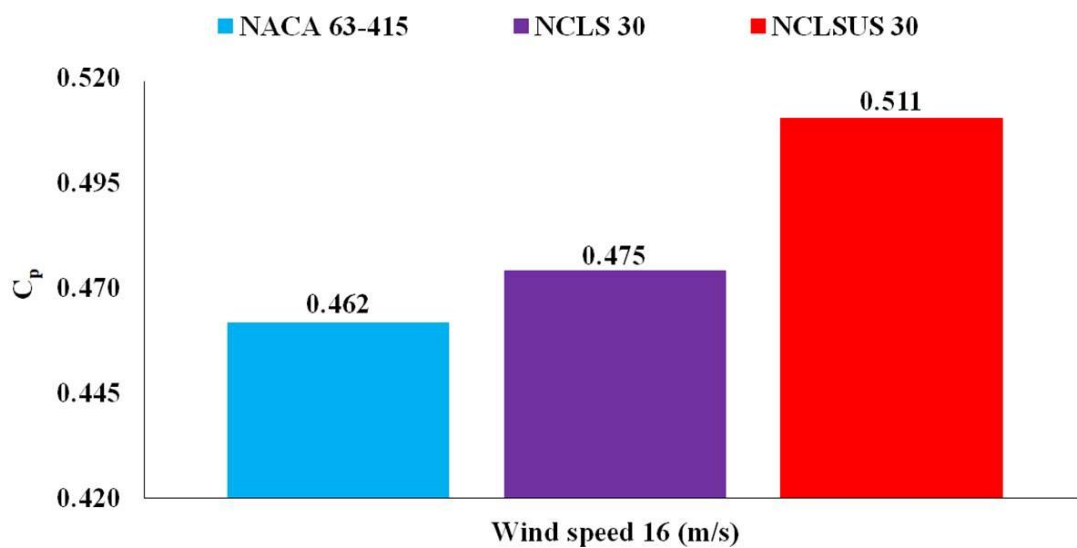

Figure 9. Comparison of C_P values of NACA 63-415, NCLS 30 and NCLSUS 30 blade models for 16 m/s wind speed

3.2 Influence of the modification of the aerofoil geometry on blade velocity distribution
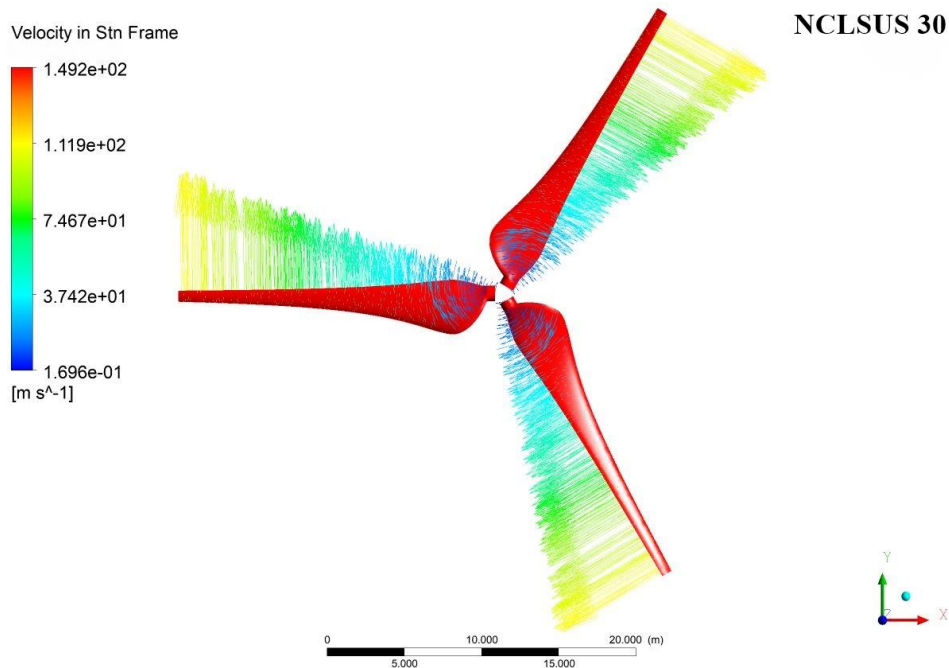
In this section, since the highest C_P value was obtained at 16 m/s wind speed in Figure 8, the impact of new blades on the blade velocity distribution throughout the blade length was investigated at this speed.
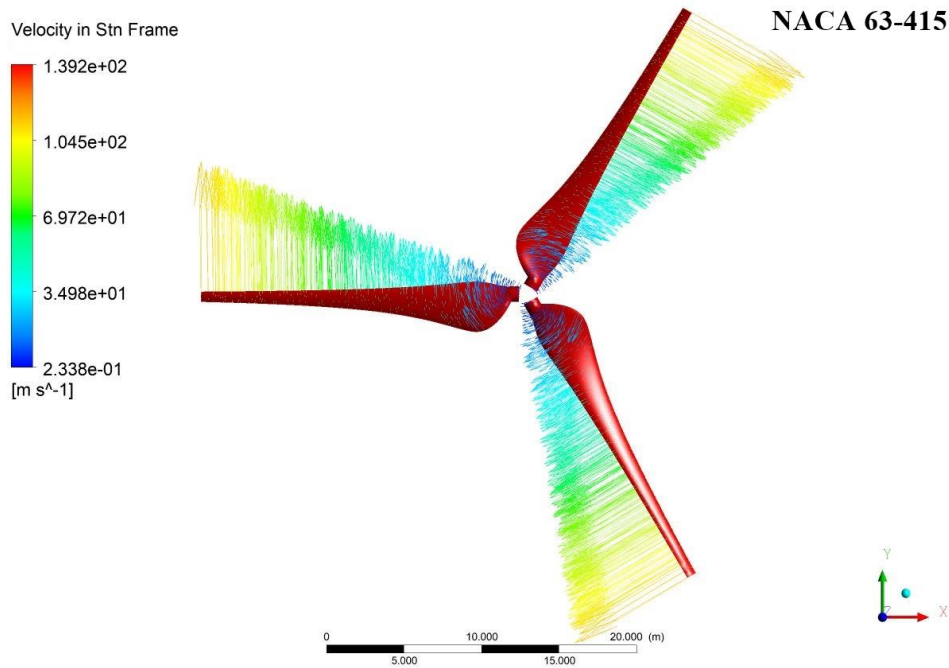
Figure 10. Distribution of velocity vector in NACA 63-415 blade
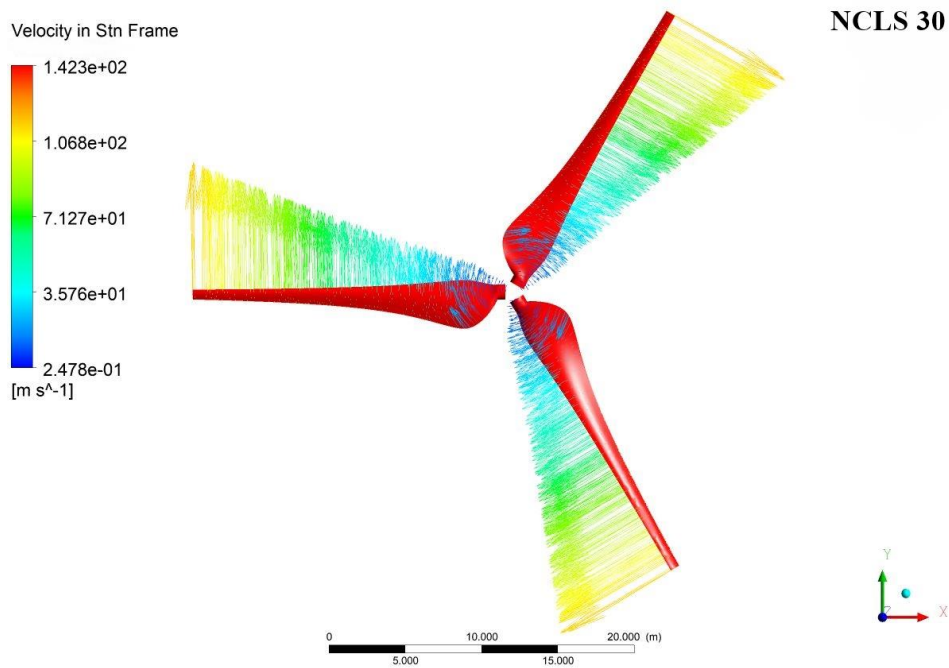
Figure 11. Distribution of velocity vector in the NCLS 30 blade

Figure 12. Distribution of velocity vector in NCLSUS 30 blade

The local blade velocity in standard frame, which is the reference frame from the ground, varies along the blade length [10, 27]. Figures 10, 11 and 12 show blade velocity distribution at 16 m/s wind speed for NACA 63-415, NCLS 30 and NCLSUS 30 blades, respectively. As expected, the blade velocity gradually increased from the blade root towards the blade tip. The velocity at the tip is the maximum for all turbine blades in Figures 10, 11 and 12.

The highest velocity at the tip of the blade are approximately 139, 142 and 149 m/s in NACA 63-415, NCLS 30 and NCLSUS 30 blades, respectively. The NCLSUS 30 blade improved the blade velocity especially in the tip region compared to other blades and the maximum blade velocity is increased by 7.2% with NCLSUS 30 blade compared to the NACA 63-415 blade.

It can be concluded that NCLSUS 30 blade produced by alteration of lower and upper surfaces of NACA 63-415 airfoil is superior to standard NACA 63-415 blade with regard to the maximum blade velocity and power coefficient improved.

5. Conclusions

In this study, the new airfoils and blades were developed to scrutinize the impacts of airfoil geometry modification on performance of a HAWT using the SOLIDWORKS and ANSYS Workbench. Based on the numerical calculations, following conclusions are made.

- The blade performance of HAWT depends on many parameters such as blade length, blade tip speed ratio, angle of attack and surface geometry.
- Changes in the lower and upper surface of the airfoil geometry improve blade performance in HAWT.
- In all blades, torque, power and C_P values increased, with an increase in wind speed.
- The highest turbine power of 1693 kW and C_P of 0.511 were obtained with NCLSUS 30 blade at a wind speed of 16 m/s.
- The NCLSUS 30 blade enhanced C_P by 10.62% compared to the standard NACA 63-415 blade.

- New blades increased the blade speed especially in the tip region resulted in improving the aerodynamic performance of HAWT.
- NCLSUS 30 blade increased the maximum blade speed at the tip by 7.2% compared to the NACA 63-415 blade.
- It is thought that the two-stage CFD method employed in wind turbine blade design in the present investigation will help future studies on the performance improvement of wind turbine blade.

Authors' Contributions

HI and MK designed the study. HI developed the model and performed the computations. Both HI and MK evaluated the results and contributed to the final manuscript. MK wrote the manuscript.

Competing Interests

The authors declare that they have no competing interests.

References

[1]. M. S. Kanca, I. N. Qader, M. N. Qadir, and K. Mediha, "Recent improvements in various renewable energies and their effects on the environment and economy: a review article," *El-Cezerî Journal of Science and Engineering*, vol. 8, no. 2, pp. 909-930, 2021.

[2]. S. Rehman, M. M. Alam, L. M. Alhems, M. M. Rafique, "Horizontal axis wind turbine blade design methodologies for efficiency enhancement—a review," *Energies*, vol. 11, no. 3 pp. 1-34, 2018.

[3]. J. P. Jensen and K. Skelton, "Wind turbine blade recycling: experiences, challenges and possibilities in a circular economy," *Renewable and Sustainable Energy Reviews*, vol. 97, pp. 165-176, 2018.

[4]. I. Gul and A. Kolip, "Parça kanatlı savonius rüzgâr türbin performansının incelenmesi," *El-Cezerî Journal of Science and Engineering*, vol. 5, no. 3, pp. 816-827, 2018.

[5]. M. O. L. Hansen, *Aerodynamics of Wind Turbine*, 2nd ed., London, UK: Earthscan, 2008, pp. 18-26.

[6]. C. G. Anderson, *Wind Turbines: Theory and Practice*, New York, USA: Cambridge University Press, 2020, pp. 34-63.

[7]. P. Å. Krogstad and J. Lund, "An experimental and numerical study of the performance of a model turbine," *Wind Energy*, vol. 15, no. 3, pp. 443-457, 2012.

[8]. W. J. Zhu, W. Z. Shen, J. N. Sørensen,, "Integrated airfoil and blade design method for large wind turbines," *Renewable Energy*, vol. 70, pp. 172-183, 2014.

[9]. C. J. Bai and W. C. Wang, "Review of computational and experimental approaches to analysis of aerodynamic performance in horizontal-axis wind turbines (HAWTs)," *Renewable and Sustainable Energy Reviews*, vol. 63, pp. 506-519, 2016.

[10]. M. Hasan, A. El-Shahat, and M. Rahman, "Performance investigation of three combined airfoils bladed small scale horizontal axis wind turbine by BEM and CFD analysis," *Journal of Power and Energy Engineering*, vol. 5, no. 5, pp. 14-27, 2017.

[11]. İ. Karasu, M. Özden, and M. S. Genç, "Performance assessment of transition models for three-dimensional flow over NACA4412 wings at low Reynolds numbers," *Journal of Fluids Engineering*, vol. 140, no. 12, 121102, 2018.

[12]. A. Aşkan and S. Tangöz, "The impact of aspect ratio on aerodynamic performance and flow separation behavior of a model wing composed from different profiles," *Journal of Energy Systems*, vol. 2, no. 4, pp. 224-237, 2018.

[13]. N. Khlaifat, A. Altaee, J. Zhou, and Y. Huang, "A review of the key sensitive parameters on the aerodynamic performance of a horizontal wind turbine using computational fluid dynamics modelling," *AIMS Energy*, vol. 8, no. 3, pp. 493-524, 2020.

[14]. A. Shourangiz-Haghighi, M. A. Haghnegahdar, L. Wang, M. Mussetta, A. Kolios, and M. Lander, "State of the art in the optimisation of wind turbine performance using CFD", *Archives of Computational Methods in Engineering*, vol. 27, no. 2, pp. 413-431, 2020.

[15]. H. E. Tanurun, İ. Ata, M. E. Canlı, and A. Acır, "Farklı açıklık oranlarındaki NACA-0018 rüzgâr türbini kanat modeli performansının sayısal ve deneysel incelenmesi," *Politeknik Dergisi*, vol. 23, no. 2, pp 371-381, 2020.

[16]. A. Eltayesh, F. Castellani, M. Burlando, M. B. Hanna, A. S. Huzayyin, H. M. El-Batsh, and M. Becchetti, "Experimental and numerical investigation of the effect of blade number on the aerodynamic performance of a small-scale horizontal axis wind turbine," *Alexandria Engineering Journal*, vol. 60, pp. 3931-3944, 2021.

[17]. I. Gov, "Rotor spacing and blade number effect on the thrust, torque, and power of a coaxial rotor," *El-Cezerî Journal of Science and Engineering*, vol. 7, no. 2, pp. 487-502, 2020.

[18]. Y. F. Gorgulu, M. A., Ozgur, and R. Kose, "CFD analysis of a NACA 0009 aerofoil at a low Reynolds number," *Politeknik Dergisi*, vol. 24, no. 3, pp. 1237-1242, 2021.

[19]. W. Yossri, S. B. Ayed, and A. Abdelkefi, "Airfoil type and blade size effects on the aerodynamic performance of small-scale wind turbines: computational fluid dynamics investigation," *Energy*, vol. 229, 120739, 2021.

[20]. B. Ji, K. Zhong, Q. Xiong, P. Qiu, X. Zhang, and L. Wang, "CFD simulations of aerodynamic characteristics for the three-blade NREL Phase VI wind turbine model," *Energy*, vol. 249, 123670, 2022.

[21]. C. V. Rodriguez and C. Celis, "Design optimization methodology of small horizontal axis wind turbine blades using a hybrid CFD/BEM/GA approach," *Journal of the Brazilian Society of Mechanical Sciences and Engineering*, vol. 44, no. 6, 254, 2022.

[22]. H. Inan and M. Kaplan, "Alt Yüzeyi Modifiye Edilmiş NACA 63-415 Kanat Profilinin Aerodinamik Performansının Sayısal Analizi," *Avrupa Bilim ve Teknoloji Dergisi*, vol. 34, pp. 121-125, 2022.

[23]. F. Bertagnolio, N. N. Sørensen, J. Johansen, and P. Fuglsang, *Wind turbine airfoil catalogue*, Denmark, Forskningscenter Risoe, Risoe-R-1280 (EN), 2001.

[24]. U. Elibuyuk and I. Uçgul, "Rüzgâr türbinleri, çeşitleri ve rüzgâr enerjisi depolama yöntemleri," *Journal of YEKARUM*, vol. 2, no. 3, pp. 1-14, 2014.

[25]. F. R. Menter, "Two-equation eddy-viscosity turbulence models for engineering applications," *AIAA Journal*, vol. 32 no. 8, pp. 1598-1605, 1994.

[26]. ANSYS FLUENT 19.2, *Theory Guide*, Ansys Inc., Canonsburg PA, USA, 2018.

[27]. M. Bakırcı and S. Yılmaz, "Theoretical and computational investigations of the optimal tip-speed ratio of horizontal-axis wind turbines," *Engineering Science and Technology, an International Journal*, vol. 21, no. 6, pp. 1128-1142, 2018.